ESD-TR-67-468

Technical Note

1967-40

The GaAs-InSb Graded-Gap Heterojunction

E. D. Hinkley
R. H. Rediker

15 August 1967

Prepared under Electronic Systems Division Contract AF 19(628)-5167 by

Lincoln Laboratory
MASSACHUSETTS INSTITUTE OF TECHNOLOGY
Lexington, Massachusetts

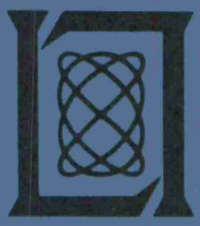

The work reported in this document was performed at Lincoln Laboratory, a center for research operated by Massachusetts Institute of Technology, with the support of the U.S. Air Force under Contract AF 19(628)-5167.

MASSACHUSETTS INSTITUTE OF TECHNOLOGY

LINCOLN LABORATORY

THE GaAs-InSb GRADED-GAP HETEROJUNCTION

E. D. HINKLEY

Group 85

R. H. REDIKER

Massachusetts Institute of Technology

TECHNICAL NOTE 1967-40

15 AUGUST 1967

LEXINGTON MASSACHUSETTS

ABSTRACT

The interface-alloy technique has been used to produce heterojunctions between GaAs and InSb. X-ray and Kossel line patterns show that, despite the relatively large 14% lattice mismatch between the semiconductors, these heterojunctions are single-crystal. Photocurrent and current-voltage measurements are explained by a model for the heterojunction band structure in which the salient feature is a region of the order of 60 Å long which has a linearly-graded energy gap joining the GaAs to the InSb. In addition, interface states "fix" the location of the GaAs bands at the heterojunction interface such that, at room temperature, the conduction band extrapolates to a value approximately 0.93 eV above the Fermi level. The photocurrent occurs via hot carriers generated in the graded-gap region which traverse this region (with a mean free path of approximately 20 Å) to the heterojunction barrier maximum. As predicted by the model, incident monochromatic radiation of energy smaller than the GaAs bandgap produces a photocurrent which varies exponentially with photon energy as $I_o \exp [C(h\nu - E_g)]$, where C is a positive parameter which decreases for increasing reverse bias on the

heterojunction, and I_o is the extrapolated response at the GaAs bandgap, which is independent of applied bias. The forward current of units fabricated with n-type GaAs varies as $\exp(qV/\eta kT)$, and, except at lower temperatures where tunneling becomes important, the values of η as a function of the GaAs impurity doping concentration can be explained in terms of the increase in the heterojunction barrier height with voltage, since part of the depletion layer potential is across the graded-gap region. Similarly, the voltage dependence of the reverse current is quantitatively explained by this model. The results of the capacitance-voltage measurements are consistent with the current-voltage and photocurrent measurements evaluated in terms of the graded-gap heterojunction model.

Accepted for the Air Force
Franklin C. Hudson
Chief, Lincoln Laboratory Office

CONTENTS

NOTATION

A	junction area (cm^2)
A^*	effective Richardson constant ($A\text{-}cm^{-2}/\ ^oK^2$)
C	junction capacitance (F)
$\mathcal{E}_o$	electric field in GaAs depletion region at interface in absence of graded-gap region (V/cm)
E_F	Fermi energy (eV)
E_g, E_g'	forbidden energy gap of GaAs, InSb (eV)
$E_g(eff)$	forbidden energy gap in graded-gap region (eV)
$h\nu$	photon energy (eV)
I, J	heterojunction current (A), current density (A/cm^2)
I_{ph}	heterojunction photocurrent per incident photon (A)
I_o	photocurrent extrapolated to GaAs bandgap (A)
k	Boltzmann constant ($eV/\ ^oK$)
ℓ	length of graded-gap region (A^o)
m^*	electron effective mass in GaAs (gm)
m_o	free electron mass (gm)
N_A,N_D	acceptor, donor impurity concentrations (cm^{-3})
q	magnitude of the electronic charge (C)
T	temperature (^oK)
V	applied bias (volts)
V_d	diffusion voltage (volts)
V_o	intercept of capacitance-voltage curve with abscissa (volts)
w	depletion layer width ($\mathring{A}$)
α	absorption coefficient (cm^{-1})
ϵ	static dielectric constant for GaAs (F/cm)

NOTATION (Cont'd)

$\zeta(n)$, $\zeta(p)$	energy separation between conduction, valence band edge and the Fermi level in bulk semiconductor (eV)
η	slope function for forward I-V characteristics
λ	mean free path of hot carriers (Å)
ρ, ρ'	net charge density in GaAs, InSb (C/cm^3)
$\phi^c(x)$, $\phi^v(x)$	energy of conduction, valence band edges (eV)
$\phi_g^c(x)$, $\phi_g^v(x)$	energy of conduction, valence band edges in graded-gap region (eV)
ϕ_m	conduction band maximum in graded-gap heterojunction (eV)
ψ	extrapolated barrier height of graded-gap heterojunction (eV)
ψ'	height of InSb conduction band edge at heterojunction interface (eV)
$\Delta\psi$	change in barrier height caused by impurity atoms contributed by the InSb to the mixed-crystal region during interface-alloying (eV)

THE GaAs-InSb GRADED-GAP HETEROJUNCTION*

I. Introduction

The properties of junctions between dissimilar semiconductors have been investigated by many researchers in the past few years. A study of the electrical characteristics of vapor-deposited Ge-GaAs heterojunctions led Anderson[1] to the conclusion that the band structure near the interface is determined by the electron affinity difference between the two bulk semiconductors. On the other hand, Van Ruyven's analysis of the photovoltaic effect in Ge-GaP heterojunctions,[2] where the lattice mismatch is much larger, indicated that the Fermi level near the interface was fixed at approximately the mid-point of the conduction and valence bands of the two semiconductors. Modification of the band structure by interface states created by a lattice mismatch had been suggested earlier by Oldham and Milnes,[3] and discussed by them in detail later.[4] L. L. Chang[5] has shown that the behavior of Ge-$GaAs_{1-x}P_x$ n-n heterojunctions can be described by the Anderson model for small values of "x" (small lattice mismatch), and by the interface-state model of Oldham and Milnes as "x" increases.

---

* Preliminary results of this investigation were presented at the Solid State Device Research Conference, Princeton, New Jersey, June, 1965.

Heterojunctions have also been fabricated by alloying techniques which utilize the difference in melting points between the two semiconductors for selective melting and regrowth.[6,7] A comprehensive review of the properties of various types of alloyed semiconductor heterojunctions has been prepared by Dale.[8] The interface-alloying technique, which involves nonequilibrium regrowth of one semiconductor from its higher-melting-point counterpart, has been used successfully to fabricate heterojunctions between several pairs of III-V semiconductors[6,9,10,11] and between Ge and Si.[12,13]

This paper is concerned with the properties of interface-alloy heterojunctions formed between GaAs and InSb. In spite of the fact that the lattice mismatch for these two semiconductors is 14%, which is substantially larger than that for any heterojunction studied previously, single crystal junctions are made both simply and reproducibly. The bandgap ratio of nearly 8:1 at room temperature is also much larger than that for any semiconductor heterojunction reported to date. The model for the band structure of the GaAs-InSb heterojunction, deduced from the dependence of photocurrent on the energy of the incident monochromatic light, is used to explain both the forward and reverse I-V characteristics as well as the differential capacitance measurements. In this model, the Fermi level at the interface is "fixed" by the many interface states, as proposed in previous analyses of heterojunctions with large lattice mismatch.[2-5] In addition, there is a region of the order of 60 Å long with a linearly-graded forbidden energy gap which joins the large-bandgap GaAs to the small-bandgap InSb.

II. Fabrication and Metallurgical Properties

Heterojunctions between wafers of GaAs and InSb were fabricated on a strip-heater in a hydrogen-argon atmosphere by the interface-alloy technique which we have described previously.[6,9] Oriented wafers of GaAs having dimensions 1.5 mm x 1.5 mm x 0.25 mm were used, with the InSb in the form of 1.0 mm diameter disks, 0.25 mm thick. Immediately prior to interface-alloying the wafers were etched in Br-methanol and rinsed with isopropyl alcohol: they were then positioned on the heater strip with the smooth B[111] GaAs surface in contact with the A [111] surface of the InSb disk. After purging the hot stage with the hydrogen-argon gas mixture, the heater strip temperature was raised until the InSb melted (525°C) and regrew from the GaAs, at which point the temperature was lowered. (The entire thermal cycle usually takes less than 30 seconds.) Because of the large lattice mismatch between these semiconductors, which tends to "discourage" single-crystal regrowth, extreme care had to be taken to insure cleanliness of the wafers and of the hot stage-gas system. Although in some instances the InSb regrowth was sufficiently perfect throughout to produce a mirror-like upper surface parallel to the [111] GaAs plane, the diatomic inversion which has been reported for InAs-GaSb interface-alloyed hetero-junctions,[14] and which is good evidence for a strong tendency toward single-crystal regrowth under relatively adverse conditions, was not observed for the GaAs-InSb couple when identical faces were mated.

Laue X-ray patterns taken of the InSb and GaAs forming the junction showed the InSb to be single-crystal and oriented identically with the GaAs substrate. Single crystallinity to more microscopic

dimensions was verified by sharp Kossel lines, characteristic of both InSb and GaAs, produced when the junction of a thin, cross-sectioned sample was bombarded with an electron beam 1.9 μ in diameter. If the junction were not a single crystal to the resolution of this Kossel micro-beam technique, then the lines produced by Bragg refraction from the crystal planes would have become diffuse or disappeared entirely. The 1.9 μ beam of electrons (accelerated by 25 kV) was also used to determine the spatial distribution of the four basic elements in the vicinity of the junction, and thus ascertain the amount of interdiffusion. The X-ray spectra emitted by this electron bombardment are characteristic of the individual elements, with an intensity proportional to the concentration of these elements. From the electron beam scan of cross-sectioned junctions, it was found that the concentration of each element decreased monotonically to zero over a distance comparable to the beam size, indicating that the chemical width of the GaAs-InSb interface-alloy heterojunction is less than 1.9 μ for the thermal fabrication cycle described above.

Several combinations of n- and p-type GaAs and InSb were used, although most of the experimental work reported in this paper concerns the n-n heterojunctions. For a simple and descriptive designation, terms such as n^{++}-n^{o} are used to label the GaAs-InSb heterojunction; the first term refers to the GaAs doping type and concentration, with the latter term describing the InSb. Table I lists the actual impurity concentrations corresponding to such designations.

In order to prepare a heterojunction for optical measurements, ohmic contact was made to the GaAs by alloying to it an appropriately-

clad (Au-Sn for n-type and Au-Zn for p-type) molybdenum tab. A 0.82 mm hole in the tab was positioned opposite the heterojunction so that illumination could be directed normal to the junction through the GaAs. An appropriately-doped In dot, alloyed to the InSb, served as the other ohmic contact.

III. Photocurrent Response and Band Structure

A. Experimental

Electro-optical measurements have been used as a tool to investigate the band details for the GaAs-InSb heterojunction. The spectral dependence of the photocurrent produced when the heterojunction is illuminated with monochromatic radiation was studied as a function of applied bias. Incident radiation from a tungsten halogen lamp was passed through a grating monochromator and mechanically chopped at 850 cps. Voltage proportional to the photocurrent was detected with a lock-in amplifier and displayed continuously as a function of incident photon energy on an x-y recorder. The spectrum of the incident photon flux was measured with an InSb photodiode operating at $77^{\circ}K$, which had previously been compared with a standard thermopile. The photocurrent data were mathematically corrected to correspond to constant incident photon flux density.

Incident light tends to bias the GaAs-InSb heterojunction in the forward direction, as with conventional p-n homojunction photodetectors. For heterojunctions fabricated with p-type GaAs, the GaAs becomes positive with respect to the InSb under illumination, while the opposite holds for those fabricated with n-type GaAs.

Figure 1 illustrates the spectral dependence of the photocurrent, at room temperature, for an n^{++}-n^{o} GaAs-InSb heterojunction at zero bias. The incident radiation is directed normal to the interface, i.e., through the GaAs. No measurable photocurrent is produced for photon energies greater than the GaAs forbidden energy gap (1.38 eV) because the GaAs thickness is much larger than the diffusion length of minority carriers (holes) generated near the incident surface. (For incident radiation in the plane of the junction a relatively constant photocurrent occurs for $h\nu > 1.38$ eV which is produced by the minority carriers generated in the GaAs within a diffusion length of the junction. It should be noted, however, that the below-the-gap response is identical with that of Fig. 1.)

For $h\nu < 1.38$ eV the photocurrent decreases exponentially with decreasing photon energy. Figure 2a illustrates data from the zero-bias curve of Fig. 1 plotted logarithmically as a function of photon energy, together with those corresponding to several other bias values. The photocurrent generally increases with reverse bias, especially at low photon energy. Furthermore, straight lines drawn through the data points corresponding to particular bias values tend to converge toward a single point near the GaAs forbidden energy gap. Figure 2b illustrates a similar dependence for an n^{+}-n^{o} heterojunction, where a wider range of applied bias was possible. The magnitude of the photocurrent for this unit, as extrapolated to the point of convergence, is approximately equal to that for the n^{++}-n^{o} unit of Fig. 2a, and represents an internal quantum efficiency of approximately one percent.

TABLE I

Semiconductor Carrier Concentrations

Symbol	GaAs	InSb
n^{++}	$n = 7 \times 10^{17} cm^{-3}$	$n = 4.5 \times 10^{18} cm^{-3}$
n^{+}	$n = 1.4 \times 10^{17}$	--
n^{o}	$n = 4 \times 10^{15}$	$n = 1.5 \times 10^{14}$
p^{+}	$p = 5 \times 10^{16}$	--
p^{++}	$p = 6 \times 10^{17}$	$p = 6 \times 10^{18}$

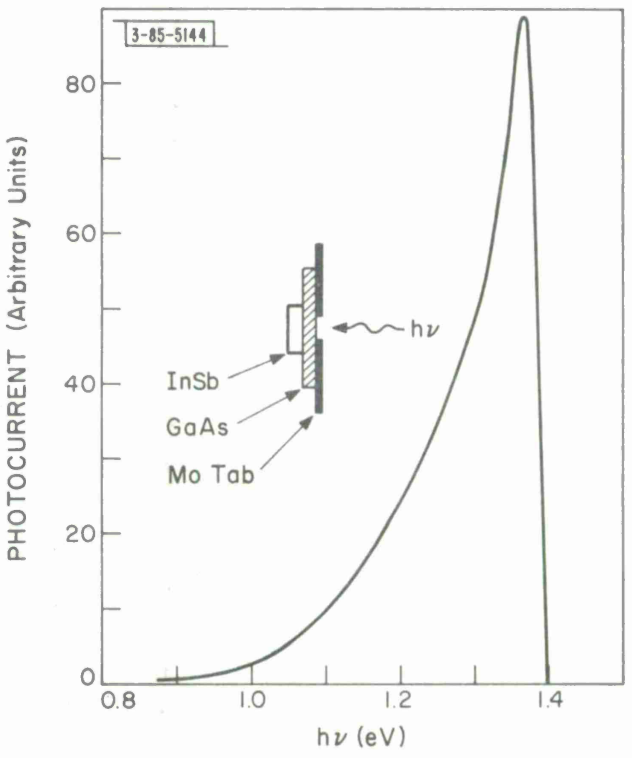

Fig. 1. Spectral distribution of photocurrent per incident photon for an n^{++}-n^{o} GaAs-InSb heterojunction at room temperature with zero applied bias. The abrupt reduction in photoresponse for $h\nu > 1.38$ eV (the bandgap of GaAs) occurs because the junction is illuminated through the GaAs which is thicker than the diffusion length of holes generated near the incident surface.

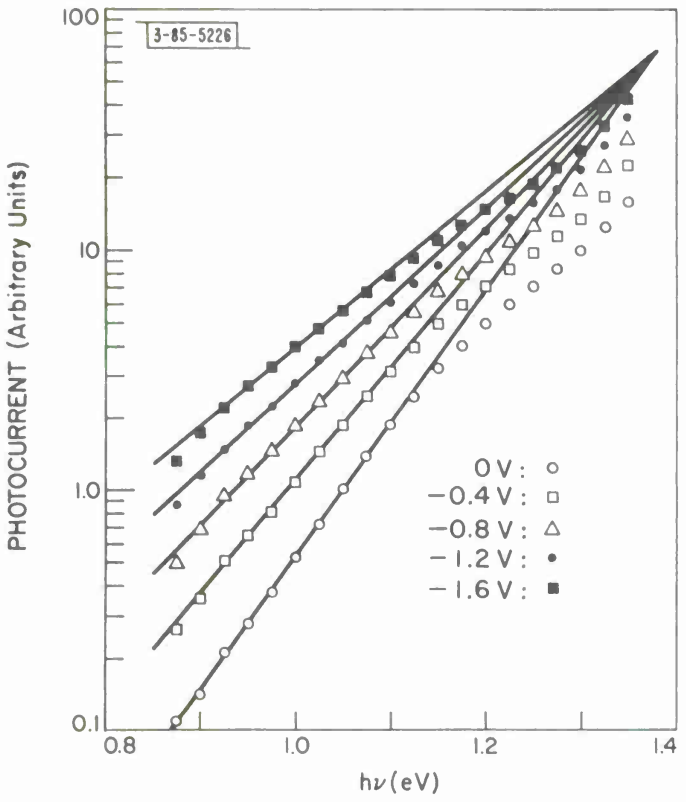

Fig. 2. Photocurrent spectra for (a) an n^{++}-n^{o} and (b) an n^{+}-n^{o} GaAs-InSb heterojunction for several values of applied bias. Solid lines drawn through linear portions of each set converge toward a common point corresponding in energy to the GaAs bandgap. Deviation of the data from linearity at high photon energies may be caused by the reduction in absorption coefficient as photon energy approaches the effective bandgap in the graded region where the photocarriers are generated (see Section C). T = 298 °K.

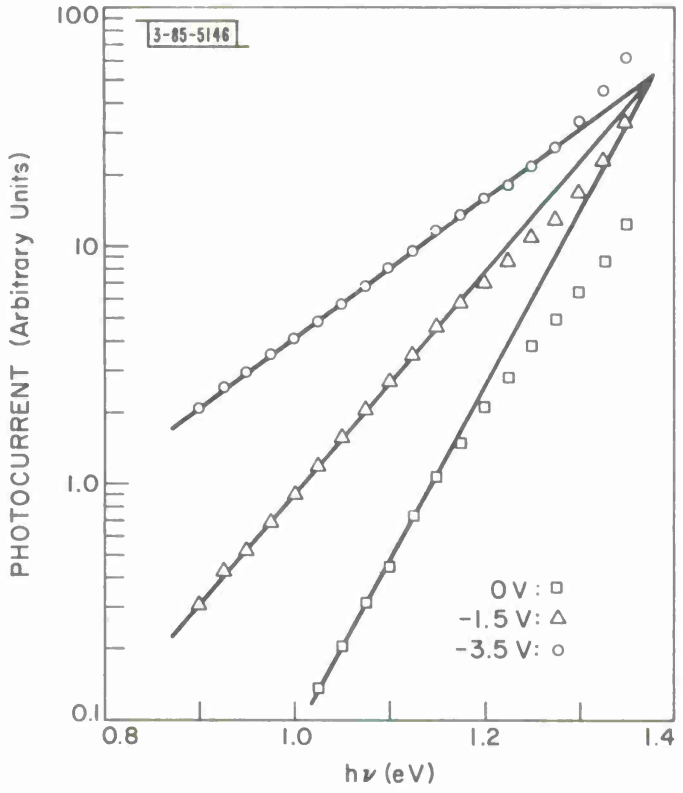

Fig. 2. Continued.

While, a priori, one might expect (on the basis of the very large bandgap difference and the small InSb bandgap) that the n-n GaAs-InSb heterojunction band structure would resemble that of a semiconductor-metal barrier, the above results, where photocurrent is exponentially related to photon energy, differ qualitatively from those reported for semiconductor-metal barriers,[15] where $I_{ph} \propto (h\nu - \psi)^2$.

B. Graded-Gap Band Model

The band model of Fig. 3 (for an n-n heterojunction) has been proposed[16] in order to explain the photocurrent results. In Sections V and VI, moreover, it will be shown that this model predicts quantitatively the current-voltage characteristics and is consistent with the capacitance-voltage measurements. Featured in this heterojunction band model is a narrow region at the interface over which the forbidden energy gap converges approximately linearly from E_g (for GaAs) to E_g' (for InSb). Created during the interface-alloying process, this graded region undoubtedly contains many traps arising from the large lattice mismatch and nonequilibrium regrowth, as well as an impurity atom concentration related to that of each of the two host semiconductors. In the model it is assumed that the electrically-active interface states are located at the boundary between the InSb and the graded region ($x = 0$), so that the values of ψ and ψ' are "fixed" at this point. The 14% mismatch between lattice constants (5.65 Å for GaAs and 6.48 Å for InSb) should create a sufficiently large number of dangling bonds to provide enough interface states to terminate the heterojunction electric field within a distance

small compared with the ~60 Å length of the graded region. Although the experimental data are sufficiently detailed to justify the graded-gap theory, they cannot yield definitive information with regard to the actual distribution of these electrically-active interface states.

C. Photocurrent Theory -- Qualitative

The mechanism by which photocurrent is produced by photon absorption in the graded-gap region may be analyzed with the aid of Fig. 3b. A photon of energy $h\nu$ is incident on the heterojunction interface in the direction shown. If $h\nu < E_g$ significant absorption will not occur until the photon reaches a point where the effective heterojunction forbidden energy gap equals the photon energy. Electron-hole pairs created by this process do not produce a photocurrent until the incident photon energy is sufficient to raise the electrons in energy to the barrier maximum. As will be discussed in detail in Section IV, this electron flow over the barrier is believed to be the limiting photocurrent process for heterojunctions fabricated with n-type GaAs, since the holes can travel easily into the InSb either directly or via recombination centers at the interface. Those electrons produced at x_1 (Fig. 3b) and traveling toward the barrier are significantly above the conduction band edge during most of their passage to ℓ, where they surmount the barrier; and as "hot" electrons they are predominantly scattered by optical phonons in polar semiconductors such as GaAs and InSb.[17] If the hot electron mean free path is defined as λ, then the probability that an electron will traverse the distance

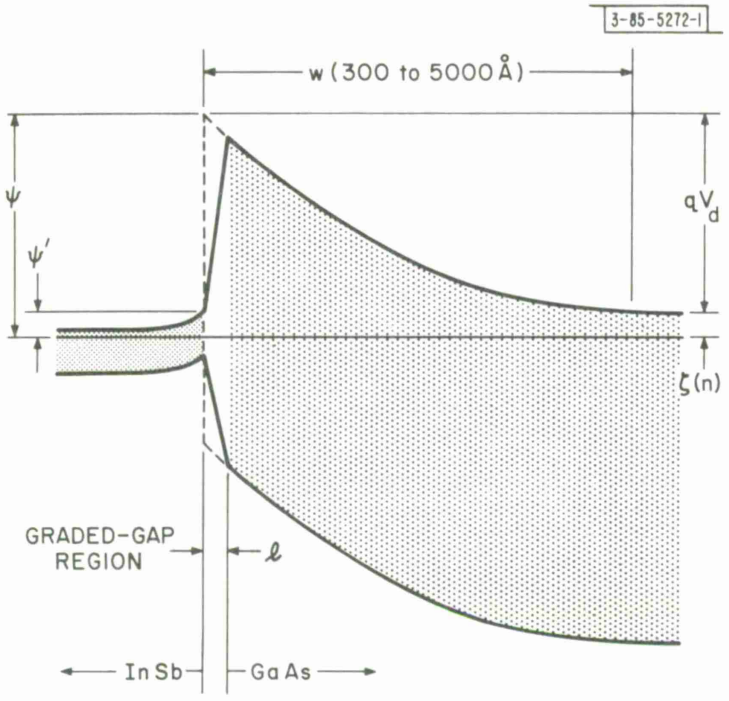

Fig. 3. (a) Proposed band diagram for n-n GaAs-InSb graded-gap heterojunction. Interface states (not shown) contain the negative charges which terminate the electric field from the depletion region. (b) An expanded view of the graded-gap region, illustrating the photocurrent mechanism at zero-bias (V_1) and reverse-bias (V_2) for a particular photon energy $h\nu$.

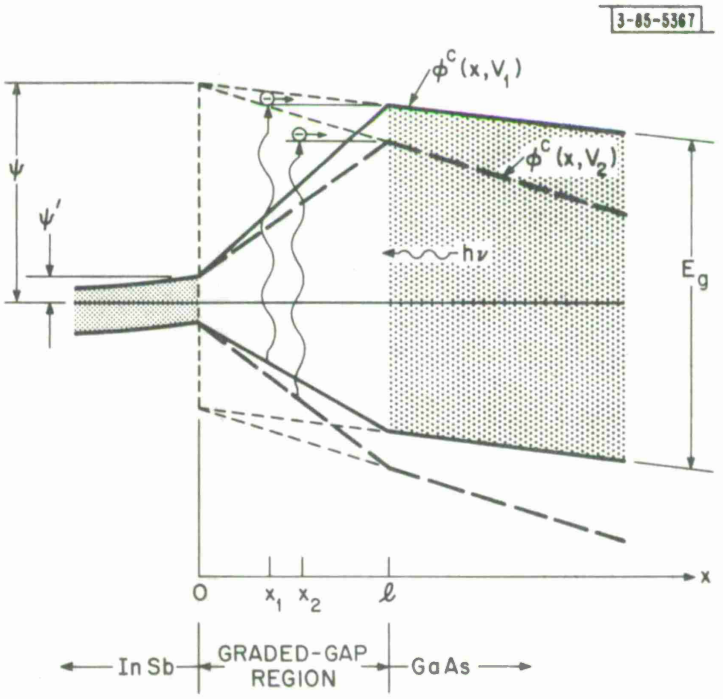

Fig. 3. Continued.

ℓ - x to the barrier maximum without being scattered is proportional to $\exp[-(\ell - x)/\lambda]$. For a linearly-graded bandgap ℓ - x is proportional to $h\nu$, and thus the model predicts an exponential decrease of the photoresponse with decreasing photon energy, as observed experimentally. Of course, those photons generating electrons at x_1 which produce the photocurrent can also generate such electrons at any point to the left of x_1 in Fig. 3b, where the gap is smaller. The effect of this contribution to the photocurrent will be discussed in Section D.

The graded-gap model also explains the experimental variation of photocurrent with applied reverse bias. As shown in Fig. 3b, the valence band edge in the graded-gap region becomes "steeper" under reverse bias; therefore, photoelectrons produced by photons of energy $h\nu$ can be generated at x_2 under reverse bias, while they could not be generated until x_1 (farther away from the barrier maximum) at zero bias. Consequently, the photocurrent is larger under reverse bias because the photoelectrons produced have a shorter path to travel to reach the barrier maximum. As the photon energy approaches E_g ,moreover, the photoelectrons are produced closer and closer to the barrier maximum, so that the influence of an external bias diminishes, in agreement with the data of Fig. 2.

D. Photocurrent Theory -- Quantitative

The spectral dependence of the photocurrent can be predicted quantitatively from the graded-bandgap model and compared with the experimental results. The spatial variation of the conduction and valence band edges is determined by solving Poisson's equation in

the region from x = 0 to x = W (see Fig. 3a), with the assumption that the interface states "fix" the barrier heights ψ and ψ' at x = 0. The graded-gap region is then introduced by superimposing a linear change in bandgap from that of InSb at x = 0 to that of GaAs at x = ℓ. For $0 < x < \ell$, the band edges are given by

$$\phi^c(x) = \psi' + (\psi-\psi') \frac{x}{\ell} - q\mathcal{E}_o x + \frac{q\rho}{2\epsilon} x^2 \equiv \phi_g{}^c(x) \qquad (1a)$$

$$\phi^v(x) = \psi' - E_g' - (E_g-E_g' - \psi+\psi') \frac{x}{\ell} - q\mathcal{E}_o x + \frac{q\rho}{2\epsilon} x^2 \equiv \phi_g{}^v(x). \qquad (1b)$$

For $x \geq \ell$,

$$\phi^c(x) = \psi - q\mathcal{E}_o x + \frac{q\rho}{2\epsilon} x^2, \qquad (1c)$$

$$\phi^v(x) = \psi - q\mathcal{E}_o x + \frac{q\rho}{2\epsilon} x^2 - E_g \quad . \qquad (1d)$$

The electric field term $\mathcal{E}_o$ is that which would exist at x = 0 in the absence of the graded region, and is defined by the relation

$$\mathcal{E}_o(V) = \left(\frac{2\rho}{\epsilon}\right)^{\frac{1}{2}} (V_d - V - kT/q)^{\frac{1}{2}} \quad , \qquad (2)$$

where V, the applied voltage, is, for reverse bias, developed across the GaAs depletion region and the graded-gap region because in this case the InSb barrier is biased in the forward direction (see Fig. 3).

For a heterojunction fabricated with n-type GaAs, so that the depletion layer is similar to that shown in Fig. 3a, the barrier over which the photoelectrons must pass in order to be captured by the

depletion field is $\phi^c(x)$ evaluated at $x = \ell$. From equation (1a),

$$\phi_m = \phi_g{}^c(\ell) = \psi - q\mathcal{E}_o\ell + \frac{q\rho}{2\epsilon}\ell^2 \quad . \tag{3}$$

The photon energy required to raise an electron from the valence band in the graded-gap region to ϕ_m is

$$h\nu = \phi_m - \phi_g{}^v(x_1) \quad . \tag{4}$$

With equation (3) for ϕ_m and (1b) for $\phi_g{}^v(x)$, equation (4) defines that point x_1 closest to the barrier maximum at which electron-hole pairs capable of producing a photocurrent are generated by photons of energy $h\nu$. If we assume that an electron generated at a distance $\ell - x$ from the barrier maximum has a mean free path λ until it reaches the maximum and is captured by the GaAs depletion field, and that $\lambda << \alpha^{-1}$ (as shown below), where α is the absorption coefficient, then the total photocurrent is proportional to

$$\alpha \int_{-\infty}^{x_1} \exp[-(\ell - x)/\lambda]\, dx = \alpha\lambda \exp[-(\ell - x_1)/\lambda] \quad . \tag{5}$$

Substituting into equation (5) the expression for $\ell - x_1$ evaluated from (4), (3), and (1b) by keeping only terms to first power in x_1 (a very good approximation for $w^2 > 10\ell^2$), we obtain the following relationship between photocurrent, photon energy, and electric field:

$$I_{ph}(h\nu, \mathcal{E}_o) = I_o \exp\left[- \frac{E_g - h\nu}{\lambda\left(q\mathcal{E}_o + \frac{E_g - E_g' - \psi + \psi'}{\ell}\right)} \right] . \tag{6}$$

Equation (6) predicts the observed exponential behavior (see Fig. 2) of photocurrent as a function of photon energy, and also that the photocurrent becomes independent of $\mathcal{E}_o$ as $h\nu \rightarrow E_g$; that is, the limiting photocurrent is I_o, which is essentially independent of either the applied bias or the GaAs impurity concentration.

At this point a short discussion of the internal quantum efficiency is necessary. The value of I_o is approximately $qN\alpha\lambda$ (where N is the incident photon flux), and thus the maximum value of the internal quantum efficiency, I_o/qN, predicted from equation (6) is approximately $\alpha\lambda$. If the mixed-crystal region of the heterojunction has absorption characteristics similar to those of GaAs and InSb, then $\alpha \approx 1\text{-}2 \times 10^4 cm^{-1}$ for photons of energy $h\nu$ generating electrons to the left of x_1 in Fig. 3b. For $\lambda = 20$ Å (see below), a maximum value of 0.4% is predicted for the internal quantum efficiency -- a result which is somewhat lower than the maximum value of approximately 1% extrapolated from the measurements, as mentioned above in Section A. Two possible explanations for this discrepancy are suggested. First, if $\alpha = 2 \times 10^4 cm^{-1}$, electrons are generated in a region extending approximately 5000 Å to the left of x_1, well into the InSb. Over much of this region these "hot" electrons have an energy significantly higher than the barrier maximum; consequently, many collisions with optical phonons are required to reduce the energy of these hot electrons below the barrier maximum, so that their effective mean free path may be considerably greater than 20 Å. The calculation of the contribution of these higher-energy carriers is further complicated by backscatter (if the carrier energy is too high when it crosses the barrier),

by the energy dependence of optical phonon scattering, and by energy loss due to impact ionization across the bandgap. No attempt, therefore, has been made to accurately calculate this contribution to the photocurrent. General agreement between theory and experiment can be retained, however, if this contribution effectively multiplies the calculated photocurrent by a constant factor, which follows from the assumption that the dependence of this factor on photon energy is much less than the exponential energy dependence of equation (6). Second, the magnitude of the absorption coefficient in the mixed crystal may actually be larger than it is for corresponding absorption in the bulk semiconductors. Finally, since α is expected to decrease as $h\nu - E_g(\text{eff}) \leq 0.1$ eV, the higher-energy photons should not produce as efficiently such "warm" electrons near the barrier maximum; this explains the fall-off from exponential behavior in Figs. 2a and 2b at high photon energy.

Differentiating $\ell n\ I_{ph}$ with respect to $h\nu$, and taking its reciprocal, yields

$$\left[\frac{d\ \ell n\ I_{ph}}{d(h\nu)}\right]^{-1} = \lambda q \mathcal{E}_o + \frac{\lambda}{\ell}\ (E_g - E_g' - \psi + \psi) \quad . \tag{7}$$

The quantity on the left hand side of equation (7) is plotted as a function of $q\mathcal{E}_o$ in Fig. 4 for the two heterojunction units of Fig. 2; results for an n^o-n^{++} GaAs-InSb unit are also shown. According to the above equation, straight lines drawn through the data should be parallel, with a slope equal to the hot-electron mean free path λ. The lines through the n^o-n^{++} and n^{++}-n^o data correspond to mean free paths of 18 and 22 Å, respectively.

Although these values for λ are smaller than the 35 Å mean free path deduced recently on the basis of avalanche multiplication experiments performed on GaAs p-n junctions,[18] this disagreement is not surprising in view of the lattice irregularities present in the graded-gap region of the heterojunction.[19] (It has, in fact, been suggested that the value of 15 Å obtained previously for GaAs from avalanche multiplication experiments can be explained by lattice irregularities in the p-n junctions used.[20]) In addition, since the average energy of the hot electrons is less in the graded-gap heterojunction than for avalanche multiplication, there would be a tendency toward smaller experimental values of λ in the former case.[21]

The n^+-n^o GaAs-InSb data of Fig. 2b and Fig. 4 are for the same unit; and although there is a deviation from linearity in the high-field region of Fig. 4, the earlier figure demonstrates a consistency with the general features of the graded-gap model. Similar results have been obtained for other units fabricated with GaAs of the same doping range, but taken from different ingots -- consequently, the deviation from linearity cannot <u>simply</u> be attributed to compensation or deep-trap effects. (The use of InSb with different impurity concentrations did not produce any noticeable change, either.) It should be noted, however, that since the <u>derivatives</u> of curves such as are shown in Fig. 2 are plotted in Fig. 4, the latter curves are very sensitive to the exact shape of the band edges in the graded gap region, and to the values of ψ and ψ' .

The straight lines of Fig. 4 intersect the ordinate at different points. One possible explanation for this variation is an impurity

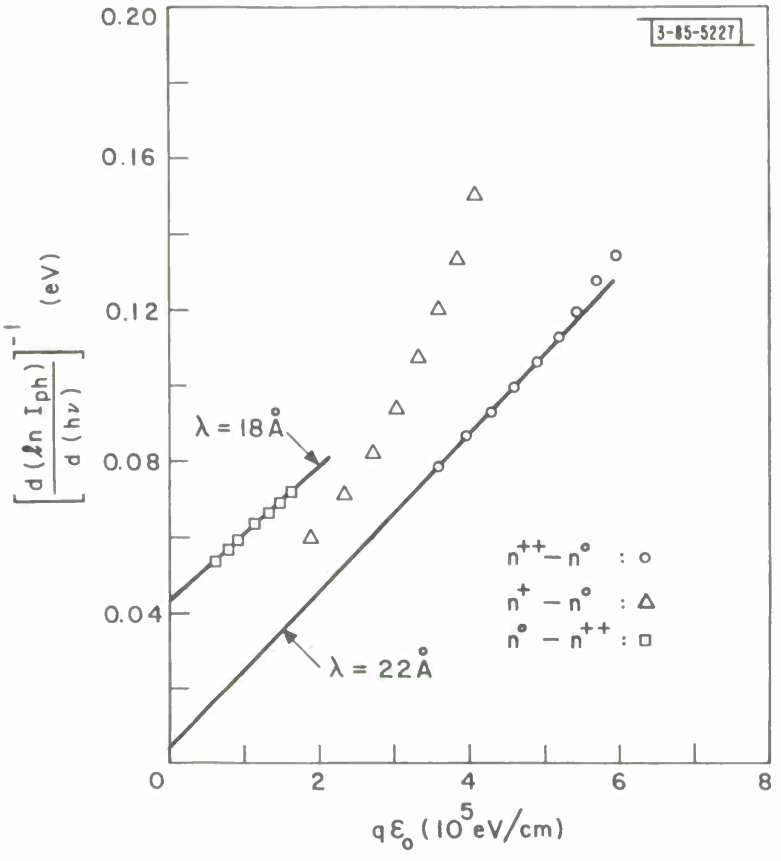

Fig. 4. The ordinate corresponds to the reciprocal slopes of experimental curves such as are shown in Fig. 2. These results are for n^{++}-n^{o}, n^{+}-n^{o}, and n^{o}-n^{++} GaAs-InSb heterojunctions at room temperature; the slopes of the straight lines in this figure are equal to the hot-electron mean free path in the graded-gap region.

charge contribution from the InSb to the graded region, an effect which has been neglected to this point. If we assume that the active impurity atom concentration in the graded-gap region varies linearly from that in the InSb to that in the GaAs, equation (7) becomes

$$\left[\frac{d\,\ell n\, I_{ph}}{d(h\nu)}\right]^{-1} = \lambda q \mathcal{E}_o + \frac{\lambda}{\ell}\,(E_g - E_g' - \psi + \psi' - 3\Delta\psi)\quad , \qquad (8)$$

where $\Delta\psi \equiv \frac{q\rho\ell}{6\epsilon}^{2}\,(1-\frac{\rho'}{\rho})$, and the "primed" terms refer to the InSb. Qualitative agreement with equation (8) has been observed by a comparison of units with the same GaAs, but different InSb impurity concentrations. However, variations in ψ and ψ' from one unit to another are nearly as large as the $\Delta\psi$ effect, so that a quantitative verification of the equation cannot be obtained.

The photoresponse of the GaAs-InSb n-n heterojunction was measured at 77°K. Because of photoionization of traps frozen out at the lower temperature, an excess photocurrent was noticeable, particularly at low photon energy. However, by simultaneously illuminating the heterojunction with a d.c. tungsten source, the photocurrent response to the chopped incident radiation became identical in all respects (except for effects caused by the shift in the GaAs absorption edge) with the room temperature measurements.

IV. Band Profiles Deduced from the Photoresponse

The measured photocurrent can be analyzed on the basis of the above theory to determine the spatial dependence of the conduction

and valence band edges in the graded-gap region. Of particular interest is any significant difference in the band profiles between units having different InSb impurity concentrations, but the same GaAs. In order to minimize the effect of the GaAs doping for this type of analysis, the heterojunctions were fabricated with the purest obtainable n- and p-type GaAs; to wafers of this GaAs were interface-alloyed n^{++}, n^{o}, and p^{++}-InSb disks.

Room temperature photocurrent data were taken at zero bias and plotted logarithmically in the manner shown in Fig. 2. The valence band edge was deduced from n-GaAs units as the electron barrier maximum ϕ_m minus the photon energy $h\nu$; the conduction band edge was obtained from p-GaAs units by adding the photon energy to the hole barrier maximum $(\phi_m - E_g)$. The spatial coordinate x_1 corresponding to a particular photon energy $h\nu$ (and hence a band edge energy) was determined from the experimental data and equation (5), which is rewritten as

$$I = I_o \exp[\, -(\ell - x_1)/\lambda\,] \,, \qquad (9)$$

where I_o is the photocurrent at the point of linear extrapolation to the GaAs bandgap, and λ the hot-carrier mean free path,* which is assumed to be 20 Å on the basis of measurements described above.

The locations of the valence and conduction band edges at x_1 with respect to the Fermi level are calculated relative to the barrier maximum ϕ_m, as mentioned above. Taking into account the contribution of the InSb impurity atoms to the charge density in the graded-gap region, equation (3) becomes

---

* Since the ionization rate parameters for holes and electrons in GaAs are nearly identical,[22] the "hot" electron and hole mean free paths are probably the same.

$$\phi_m - \psi - [q\mathcal{E}\ell - q\rho\ell^2/2\epsilon - \Delta\psi] \quad . \tag{10}$$

For units fabricated with n-type GaAs, in which the photocurrent occurs via electrons originating at the valence band edge,

$$\phi_g^{v}(x_1) = \phi_m - h\nu \quad . \tag{11a}$$

For p-GaAs units, in which the photocurrent occurs via holes, by analogy, originating at the conduction band edge,

$$\phi_g^{c}(x_1) = \phi_m - E_g + h\nu \quad . \tag{11b}$$

Band profiles deduced in the above manner from the photocurrent are shown in Figs. 5a, 5b, and 5c for n^{++}-, n^{o}-, and p^{++}-InSb heterojunctions, respectively. A value of 0.93 eV is assumed for the barrier height ψ in equation (10) -- this represents the average from I-V and C-V measurements on the GaAs-InSb heterojunctions (see sections V and VI), and is in agreement with the results for metal--n-GaAs barriers.[15] The small correction term ($\sim$5%) in the brackets of equation (10) was calculated assuming ℓ = 60 Å. Linearity of the bands over a large portion of the mixed-crystal region supports the basic assumption of a linearly-graded bandgap. The straight lines drawn through the data converge from a bandgap of 1.38 eV to 0.18 eV in a distance of 75 to 80 Å. The consistency of the three sets of band profiles is believed to be significant since only two parameters (ψ and λ) have any large influence on the results. The probable band configuration for the InSb, which has been compressed horizontally for clarity, is indicated by the dashed lines.

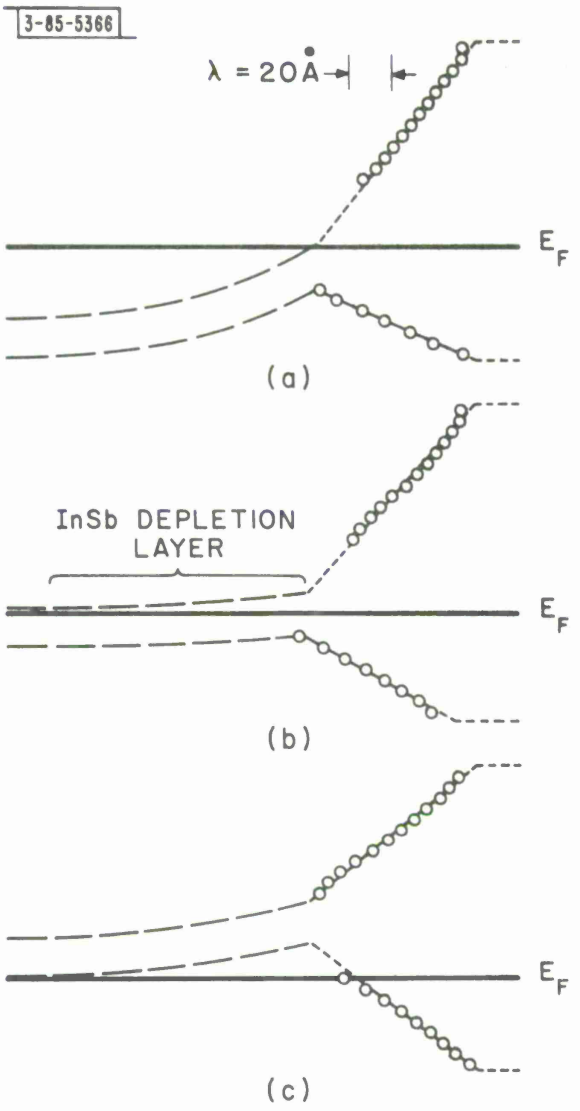

Fig. 5. Detailed band structure in the graded-gap region of GaAs-InSb heterojunctions at zero applied bias, as deduced from electro-optical measurements, illustrating the influence of the InSb doping concentration. Straight lines through the data points indicate a distance of 75 to 80 Å for gap convergence from 1.38 to 0.18 eV. Parameters used: $\lambda = 20$ Å, $\psi = 0.93$ eV. The probable band configuration for the InSb, which has been compressed for clarity, is indicated by the dashed lines.

One important assumption in this paper is that the limiting photocurrent process is the hot carrier flow over the barrier Φ_m. As shown in Fig. 5 for n-type GaAs, there is, in addition to the barrier which the hot electrons must surmount, a "notch" in the valence band at the interface between the graded region and the InSb, which can trap holes produced in this region. Indeed, Anderson has shown[23] that the presence of a "notch" in the conduction band of the Ge-GaAs heterojunction profoundly influences its electro-optical response. However, the number of interface states in the Ge-GaAs heterojunction, with its lattice mismatch of 0.1%, is much smaller than it is for the GaAs-InSb heterojunction, which has a 14% lattice mismatch. Calculations have shown that interface states in large-mismatch heterojunctions can cause severe minority carrier recombination;[4] thus, in Figs. 5a and 5b, the holes, rather than becoming trapped in the "notch," recombine with electrons at the interface and thereby produce electron flow in the n-type InSb. For heavily-doped p-type InSb, illustrated in Fig. 5c, the degeneracy at the interface prevents the "notch" from trapping the majority-carrier holes.

Three experimental findings support the assumption that the limiting photocurrent process is hot carrier flow over the barrier rather than trapping in the "notch." First, the results for units with n-type GaAs are similar in detail to those for units with p-type GaAs for which, as shown in Fig. 5, there is no notch to trap the electrons produced in the graded gap region. Second, the photocurrent for the n-n units at $77^{\circ}K$ is essentially identical to that measured at room temperature, and thus is not limited by

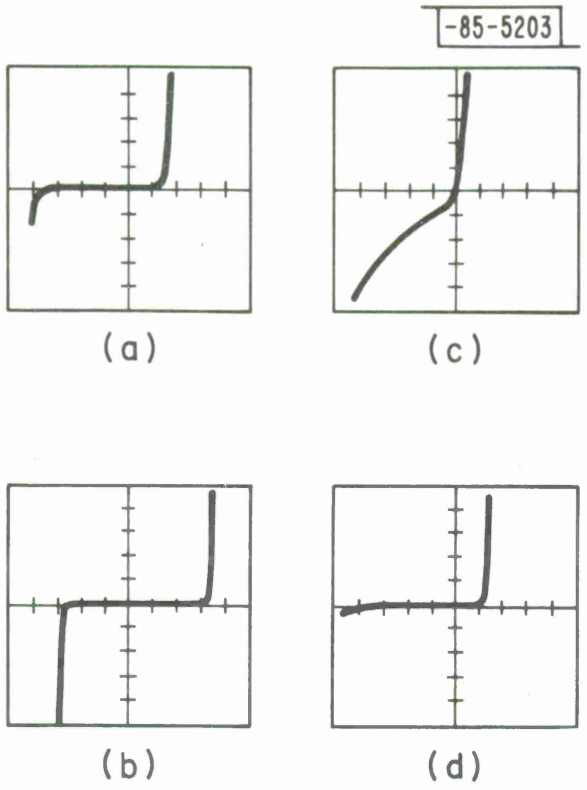

Fig. 6. Current-voltage characteristics of two representative GaAs-InSb heterojunctions: an n^{o}-n^{++} unit at room temperature (a) and 77° K (b); a p^{+}-p^{++} unit at room temperature (c) and 77° (d). Forward bias scale is 0.2 V/division in all figures. Reverse bias scale is 10 V/division for (a) and (b), and 0.2 V/division for (c) and (d). Current scale (vertical) is 10 μA/division in all figures, except for (c) where it is 1 mA/division. Avalanche breakdown occurs at −40 V in (a) and at −28 V in (b).

a barrier to thermalized carriers. Third, no radiative recombination (corresponding to either the InSb or GaAs bandgaps) is observed when p-n or n-p GaAs-InSb units at liquid helium temperatures are pulsed with forward current densities to 6000 A/cm^2.

V. Current-Voltage Characteristics

The I-V characteristics of two GaAs-InSb heterojunctions are shown in Fig. 6. The n^o-n^{++} unit of Fig. 6a has a room-temperature rectification ratio of 1×10^8 at 0.5 volts. Avalanche breakdown occurs at a reverse bias of 40 volts, compared with a theoretical maximum of approximately 70 volts computed numerically by Sze and Gibbons[22] for a GaAs p-n junction of similar impurity concentration. At 77^oK the voltage at avalanche is smaller (Fig. 6b) because a longer mean free path at this lower temperature[18] allows the carriers to achieve the necessary ionization energy in a smaller electric field.[24] The I-V characteristics of a p^+-p^{++} unit at room temperature are shown in Fig. 6c. The relatively poor rectification is a direct consequence of a small barrier to charge flow in the valence band; and, as expected, rectification is improved at 77^oK (Fig. 6d).

As in the metal-semiconductor "Schottky" barrier, the current in an n-n GaAs-InSb heterojunction is due to majority carrier flow across a barrier, and in the forward direction it varies as $\exp(qV/\eta kT)$ over a wide range of applied bias. Values of η greater than unity can usually be explained by one or more of the following mechanisms: (a) image-force lowering of the potential barrier,[25] (b) tunnel penetration of the barrier by the charge carrier,[26] (c)fluctuations of the contact potential over the

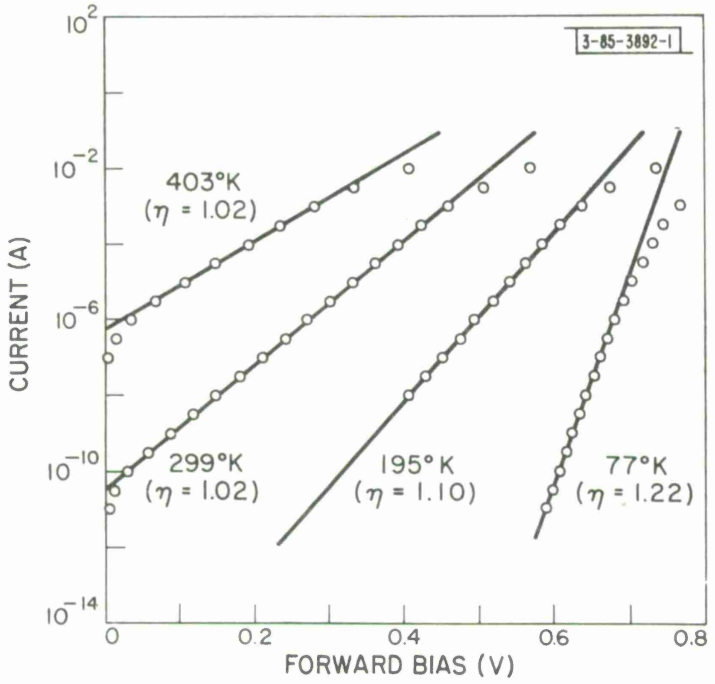

Fig.7. Forward current-voltage characteristics of n^{o}-n^{++} GaAs-InSb heterojunction at several ambient temperatures. Deviation from linearity at high currents is caused by series resistance effects. The quantity η is defined by the relation $I = I_{o} \exp(qV/\eta kT)$.

barrier region,[25,26] (d) presence of a graded-gap region at the interface,[16] and (e) distribution of the applied voltage between the two semiconductors which comprise the heterojunction.[5] The electro-optical measurements described above indicate the presence of a graded-gap region at the GaAs-InSb interface; and it will be shown that this graded-gap model predicts the observed forward and reverse I-V characteristics at room temperature and above; at low temperatures tunneling becomes dominant. As described above in reference to equation (2), our model predicts that for reverse bias essentially all of the applied voltage is developed across the GaAs and the graded region. Capacitance-voltage measurements indicate that for all the heterojunction units studied this is also true for forward bias, except for n^{o}-InSb units below room temperature, as will be discussed in Section VI.

Figure 7 is a semilogarithmic plot of the forward I-V characteristics of an n^{o}-n^{++} GaAs-InSb heterojunction at several ambient temperatures from 403 to 77°K. The straight lines through the data correspond in slope to values of η from 1.02 at room temperature and above (corresponding to thermal emission of electrons over a graded-gap-reduced barrier) to 1.22 at 77°K (where tunnel injection becomes significant). According to Bethe's development[25] for thermal emission of charge carriers over a barrier of height ϕ_m, the current density may be written as

$$J = A^{*}T^{2}e^{-\phi_m/kT}\left[e^{qV/kT} - 1\right], \qquad (12)$$

where $T(^{o}K)$ is the junction temperature and $A^{*}(A\text{-}cm^{-2}/^{o}K^{2})$ the effective Richardson constant.[27] If the barrier height ϕ_m were independent of applied bias, then the forward I-V slope would correspond to $\eta = 1$, with the reverse current density saturating at the value $A^{*}T^{2}\exp[-\phi_m/kT]$. Neither of these conditions has actually been observed for the GaAs-InSb n-n heterojunction, although values of η very close to unity have been measured for units fabricated with relatively pure GaAs.

In order to evaluate the forward I-V characteristics in terms of the graded-gap model, we use the expression for ϕ_m obtained by substituting for $\mathcal{E}_o$ in equation (3) and expanding to first order in V (a good approximation at room temperature and above, where $V << 2V_d \approx 1.5$ volts):

$$\phi_m \approx \psi - q\left(\frac{2\rho V_d}{\epsilon}\right)^{\frac{1}{2}} \ell + \frac{q\rho\ell^2}{2\epsilon} + q\left(\frac{\rho}{2\epsilon V_d}\right)^{\frac{1}{2}} \ell V \quad , \tag{13}$$

where we have justifiably neglected kT/q which is $<< V_d$. Neglecting the "-1" term in equation (12), the forward current density becomes

$$J \approx J_o \exp\left[\frac{q}{kT}\left(\frac{2\rho V_d}{\epsilon}\right)^{\frac{1}{2}} \ell\right] \exp\left(\frac{qV}{\eta kT}\right) \tag{14}$$

where

$$J_o \equiv A^{*}T^{2} \exp\left[-(\psi + q\rho\ell^2/2\epsilon)/kT\right], \tag{14a}$$

and η is related to the graded-gap length by

$$(1 - 1/\eta) = (\rho/2\epsilon V_d)^{\frac{1}{2}} \ell \quad . \tag{15}$$

The diffusion voltage V_d may be obtained from capacitance-voltage measurements discussed below. Measurements of the forward I-V characteristics show, as expected from equation (15), that η varies with the GaAs impurity concentration. In Fig. 8 are plotted the room-temperature values of $(1-1/\eta)$ for three units having different GaAs impurity concentrations. At this temperature, and for these concentrations and bias conditions, tunneling is presumed to be negligible, with the deviation of η from unity due to the increase of barrier height with voltage, as predicted by the graded-gap model. Using equation (15), the slope of a straight line through these data and intersecting the origin corresponds to a graded-gap length of approximately 64 Å.

Since η is usually quite close to unity, it is obvious from equation (15) that determination of the graded-gap length from the forward I-V slope can be very inaccurate. A much better value is obtained from the reverse I-V characteristic. Under reverse bias such that the first term in the brackets of equation (12) can be neglected, and using equation (3) for ϕ_m, the heterojunction current density becomes

$$J = -J_o \exp\left[\left(\frac{q}{kT}\right)\left(\frac{2\rho}{\epsilon}\right)^{\frac{1}{2}} \ell \left(V_d - V - \frac{kT}{q}\right)^{\frac{1}{2}}\right], \qquad (16)$$

where J_o is the same as that in equation (14). A plot of $\ell n\ J$ vs. $(V_d - V - kT/q)^{\frac{1}{2}}$ should be linear with slope $\frac{q}{kT}\left(\frac{2\rho}{\epsilon}\right)^{\frac{1}{2}} \ell$ and intercept J_o. Figure 9 illustrates this type of dependence for three units of different GaAs impurity concentration. (The ambient temperature of approximately 400°K insures the predominance of

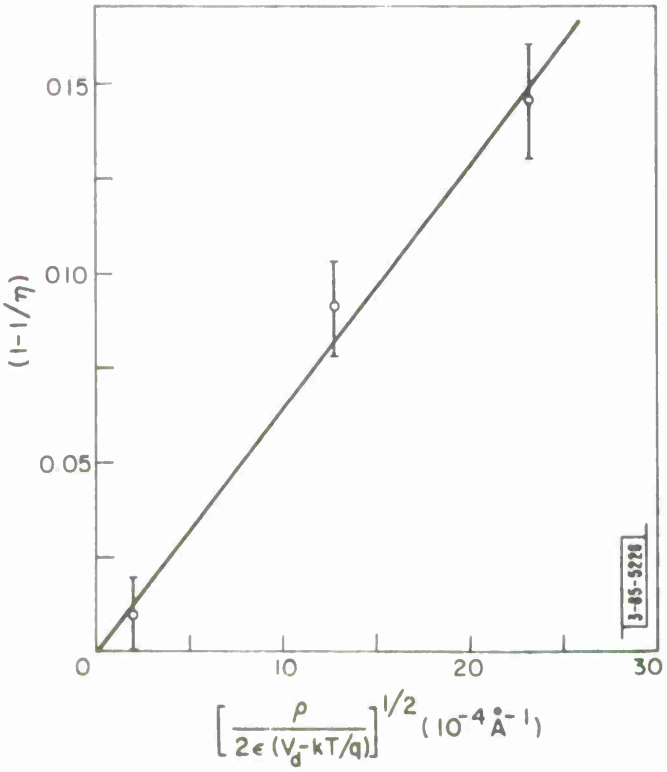

Fig. 8. Illustrates a determination of the graded-gap length ℓ from room-temperature values of η. Error bars indicate the uncertainty in the ordinate values. Using equation (15), the straight line corresponds to an average graded-gap length of approximately 64 Å. The diffusion voltages for the three units used were deduced from the capacitance-voltage measurements.

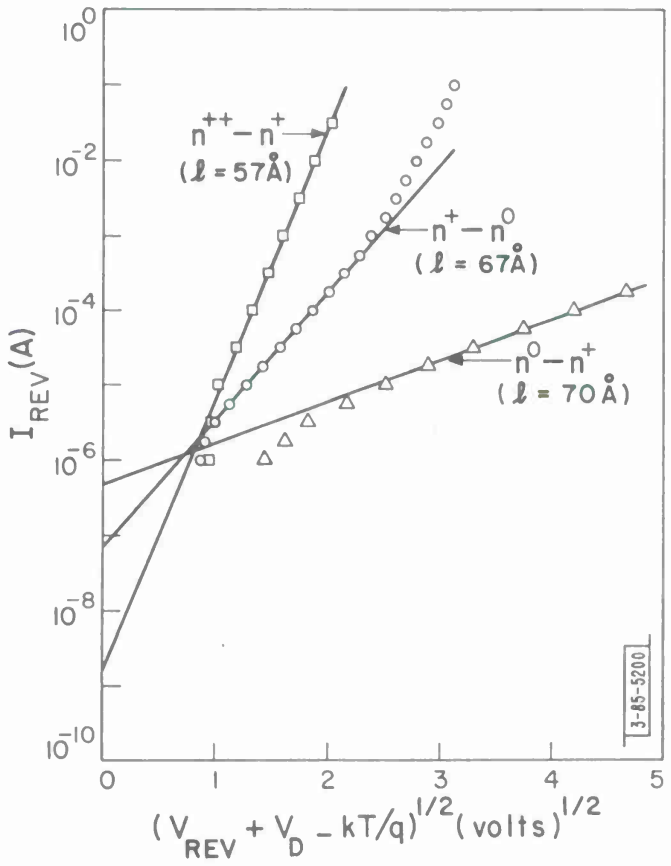

Fig. 9. Reverse current vs. net barrier voltage for three n-n GaAs-InSb heterojunctions at 400° K. Linearity of curves over a large portion of the reverse characteristics is in qualitative agreement with equation (16); the slopes correspond to the graded-gap lengths indicated. Diffusion voltages and junction areas are: 0.89, 0.78, and 1.89 eV, and 33, 98, and 51×10^{-4} cm^2 for the n^{++}-n^{++}, n^+-n^o, and n^o-n^{++} units, respectively.

TABLE II

Heterojunction Parameters Deduced from
Current- and Capacitance-Voltage Measurements

GaAs Designation	Graded-Gap Length, (Å)		Barrier Height, (eV) at 400°K		
	From Reverse I-V Slope	From Forward I-V Slope	From Reverse I-V Intercept	From Forward I-V Intercept	From Capacitance Intercept
n^{++}	57	44	0.96	0.95	0.94
n^{++}	65	56	0.97	0.97	0.92
n^{+}	67	67	0.88	0.88	0.85
n^{+}	75	91	0.91	0.90	0.86
n^{o}	91	40-270*	0.84	0.83	0.87
n^{o}	70	80-230*	0.82	0.82	0.90

(* Large variation in these values stems from uncertainty in slope determination.)

thermal emission over tunneling.) The values for ℓ obtained from the slopes of these curves are 57, 66, and 70 Å for the n^{++}-n^{++} n^{+}-n^{o}, and n^{o}-n^{++} GaAs-InSb-units, respectively; and the intercepts, using equation (14a), yield barrier heights ψ of 0.96, 0.88, and 0.82 eV. The graded-gap lengths appear to be in general agreement with those obtained from the photocurrent and forward I-V measurements. Furthermore, since ℓ can be more accurately determined from the reverse characteristics than from the other two measurements, the variations from unit to unit are probably real.

Table II shows the graded-gap parameters as deduced from the forward and reverse I-V measurements, as well as the C-V measurements, for several heterojunction units at approximately 400°K. These units are labeled only by their GaAs impurity concentration for simplicity, since any variations in the I-V or C-V data produced by InSb of different impurity concentrations is smaller than the usual variations from one "identical" unit to another. It should be noted, moreover, that barrier height determinations for a particular unit are consistent.

The current-voltage characteristics determined rigorously from equations (12) and (10) are compared with the experimental data in Figs. 10a and 10b for an n^{+}-n^{o} and n^{++}-n^{o} GaAs-InSb heterojunction, respectively. The points correspond to the experimental data, and the solid curves to the theoretical prediction on the basis of two adjustable parameters for each unit: ℓ = 65 and 67 Å; ψ = 0.97 and 0.88 eV, for (a) and (b), respectively. (From capacitance-voltage measurements the respective barrier heights are 0.91 and 0.85 eV.) At large reverse bias the measured current for these two units is larger than its predicted value because of tunneling

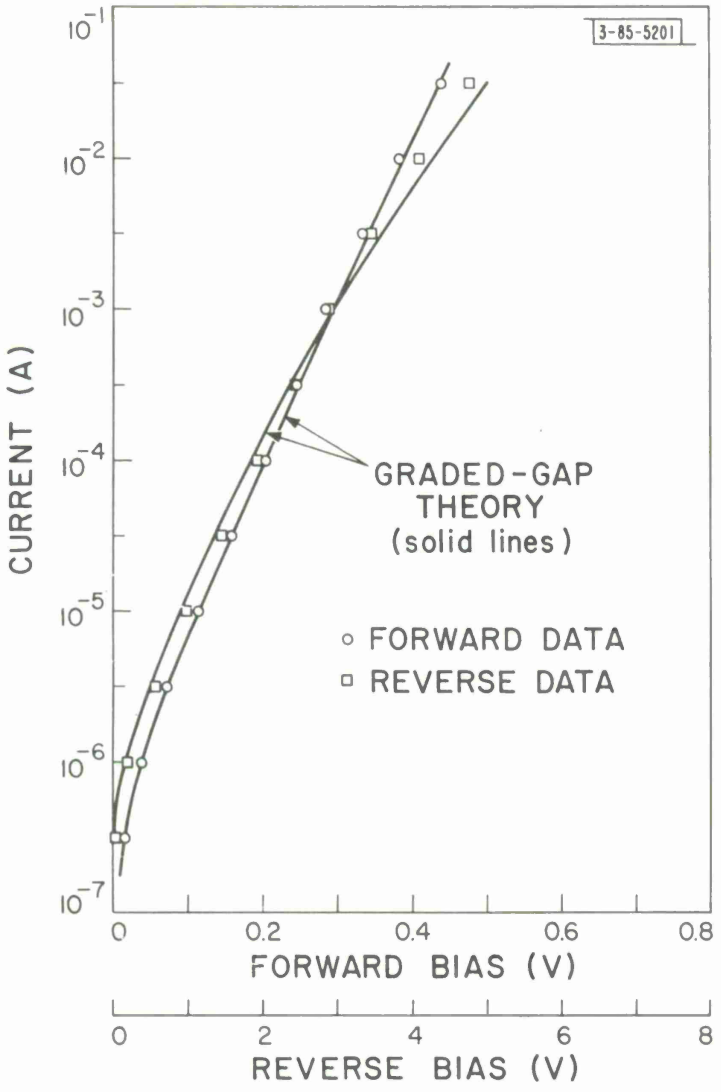

Fig. 10. Comparison between theory (solid lines) and experiment (points) for forward and reverse current-voltage characteristics of (a) an n^{++}-n^{o} and (b) an n^{+}-n^{o} GaAs-InSb heterojunction at 388 and 396°K, respectively. Identical voltage scales permit direct comparison between the two units. Adjustable parameters are: $\ell = 65$ Å, $\psi = 0.97$ eV for (a); and $\ell = 67$ Å, $\psi = 0.88$ eV for (b).

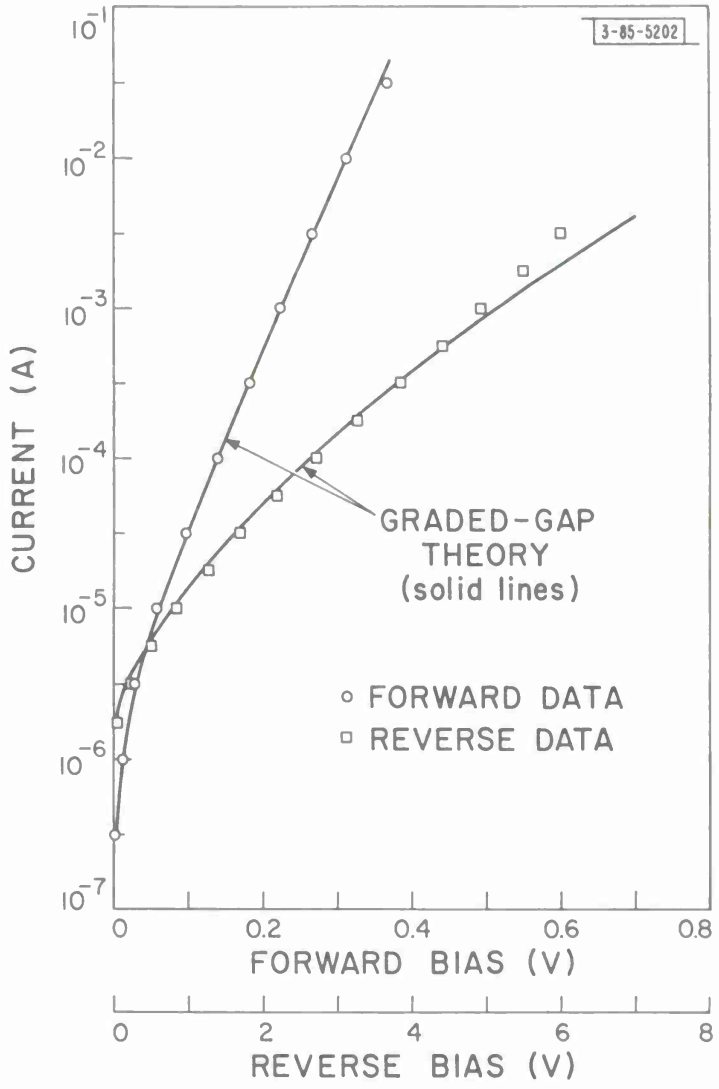

Fig.10. Continued.

of the electrons through the narrow graded-gap barrier. Units involving n^{o}-InSb, however, reach avalanche (see Figs. 6a and 6b) before substantial tunneling occurs.

VI. Capacitance-Voltage Characteristics

The capacitance of the GaAs-InSb heterojunctions, measured as a function of applied bias with a 100 kHz bridge, varies inversely as the square root of the net barrier potential and depends on the GaAs impurity concentration. If the junction capacitance of the graded-gap model of Fig. 3a is developed in accordance with Goodman's analysis[28] for a metal-semiconductor barrier, the slope of a C^{-2} vs. V plot for the GaAs-InSb heterojunction is

$$\frac{d(C^{-2})}{dV} = - \frac{2}{A^2 \rho \epsilon} \quad , \tag{17}$$

where A is the junction area. The intercept V_o at the abscissa is given by

$$V_o = V_d - kT/q = \psi - \zeta(n) - kT/q, \tag{18a}$$

$$V_o = V_d - kT/q = E_g - \psi - \zeta(p) - kT/q \tag{18b}$$

for units fabricated with nondegenerate n- and p-type GaAs, respectively. From the values of V_o obtained as a function of temperature, equation (18) can be used to deduce the temperature dependence of the heterojunction barrier height ψ . For n-GaAs heterojunctions, ψ increases with decreasing temperature at a rate equal to that for the GaAs forbidden energy gap, and has a room-temperature value of approximately 0.93 eV. Conversely, units

fabricated with p-type GaAs show a temperature-independent barrier height of approximately 0.59 eV. These results agree with those of Mead and Spitzer for Au-GaAs barriers.[29]

Although we have found that the slopes of the C^{-2}-V curves are usually equal for the forward and reverse bias conditions, two interesting exceptions have been observed. Figure 11 illustrates the C-V data of a heterojunction fabricated with n^{o}-GaAs. The forward-bias slope corresponds to an impurity concentration of $4 \times 10^{15} cm^{-3}$, which is equal to that in the bulk GaAs as measured by the Hall coefficient. The reverse-bias slope, however, corresponds to a larger concentration of $1 \times 10^{16} cm^{-3}$. Similar results were observed by Goodman[28] for metal-CdS barriers; and the different slopes were attributed to shallow traps in the semiconductor depletion layer which are ionized during reverse bias, but filled during forward bias. The small extension of the forward-bias slope into the reverse regime (Fig. 11) was achieved by switching the heterojunction from a forward bias condition to the appropriate reverse-bias state and measuring the capacitance during the one or two second interval before the traps became ionized.

The second exception to the equality of the forward and reverse slopes of the C^{-2}-V curves occurs for heterojunctions fabricated with n^{o}-InSb. Although these units behave normally at room temperature, it is consistently observed that the C^{-2}-V measurements at $77^{o}K$ produce a smaller forward-bias slope (or larger forward intercept) than that extrapolated from the reverse-bias curve. It is evident from Fig. 5b that heterojunctions fabricated with n^{o}-InSb may exhibit back-to-back diode characteristics under certain conditions. The different forward and reverse slopes of the C^{-2}-V curves of these diodes at low temperatures are a manifestation of

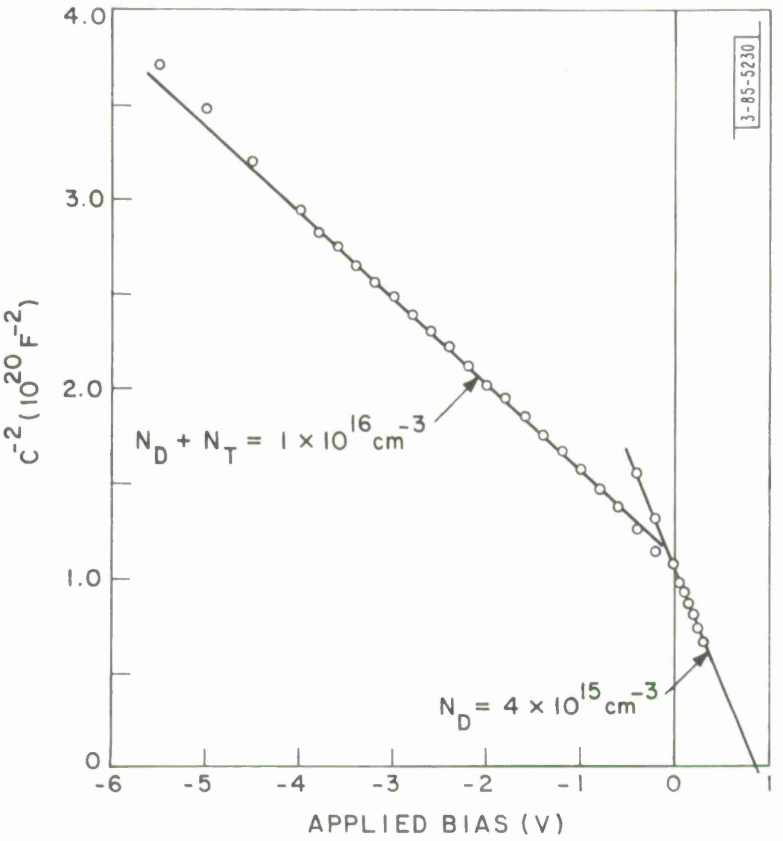

Fig. 11. Capacitance-voltage dependence of an n^{o}-n^{++} GaAs-InSb heterojunction at room temperature, illustrating large difference between forward- and reverse-biased slopes caused by the presence of shallow traps ionized in the reverse regime. Extension of the forward-biased slope into the region for which $V < 0$ was obtained from data taken before the traps became ionized.

the fact that in the "forward" direction there is a reverse-biased depletion region in the InSb across which part of the applied voltage is developed. Measurements involving units fabricated with heavily-doped p- or n-type InSb show identical forward and reverse slopes even at 77°K (except for the trap effect for n°-GaAs units, mentioned above), in agreement with the implications of Figs. 5a and 5c.

VII. Conclusion

The interface-alloy technique has been successful in producing single-crystal graded-gap heterojunctions between InSb and GaAs, despite the relatively large lattice mismatch between these two compound semiconductors. Electron beam microprobe analysis cannot resolve the extent to which the four elements involved have inter-diffused, but shows that the interdiffusion is less than 1.9 μ. Furthermore, electro-optical and current-voltage measurements indicate the presence of a graded-gap region of 60 to 80 Å at the interface. Photocurrent occurs via hot carriers generated in the graded-gap region, which traverse this region with a mean free path of approximately 20 Å to the heterojunction barrier maximum. The graded-gap model predicted by the photocurrent measurements explains quantitatively the current-voltage characteristics with only two adjustable parameters: the graded-gap length and extra-polated barrier height. The barrier heights obtained from the forward and reverse I-V characteristics and the capacitance-voltage data are in good agreement; and are also in agreement with previous results for metal-GaAs junctions. An approximate barrier height of 0.89 eV is indicated for an n-GaAs heterojunction at 400°K;

this value increases with decreasing temperature at a rate equal to that for the GaAs bandgap itself. Differential capacitance measurements performed on p-GaAs heterojunctions indicate a temperature-independent barrier height of 0.59 eV.

Acknowledgements

We thank G. A. Ferrante for performing the heterojunction fabrication as well as many of the experiments, W. H. Laswell for material preparation, M. C. Finn and M. C. Lavine for the electron beam microprobe and Kossel-line analyses, and Dr. J. O. Dimmock for several enlightening discussions.

REFERENCES

1. R. L. Anderson, Solid-State Electron. 5, 341 (1962).
2. L. J. Van Ruyven, Phys. Stat. Sol. 3, K109 (1964).
3. W.G. Oldham and A.G. Milnes, Solid-State Electron. 6, 121 (1963).
4. W.G. Oldham and A.G. Milnes, Solid-State Electron. 7, 153 (1964).
5. L. L. Chang, Solid-State Electron. 8, 721 (1965).
6. R. H. Rediker, S.Stopek, and J. H. R. Ward, Solid-State Electron. 7, 621 (1964).
7. N. K. Kiseleva, Soviet Phys. - Crystallography 9, 365 (1964).
8. J.R. Dale, Phys. Stat. Sol. 16, 351 (1966).
9. R. H. Rediker, S.Stopek, and E.D. Hinkley, Trans. Met. Soc. AIME 233, 463 (1965).
10. E.D. Hinkley, R. H. Rediker, and D. K. Jadus, Appl. Phys. Lett. 6, 144 (1965).
11. R.S. Mroczkowski, M.C. Lavine, and H. C.Gatos, Trans. Met. Soc. AIME 233, 456 (1965).
12. W. Lindley, Thesis, Purdue University, 1966.
13. J. Shewchun, Phys. Rev. 141, 775 (1966).
14. E.D. Hinkley, R. H. Rediker, and M.C. Lavine, Appl. Phys. Lett. 5, 110 (1964).
15. W.G. Spitzer and C.A. Mead, J. Appl. Phys. 34, 3061 (1963).
16. E.D. Hinkley and R. H. Rediker, Solid-State Dev. Res. Conf. Princeton (1965).
17. C. Herring, Bell Syst. Tech. J. 34, 237 (1955).
18. C.R. Crowell and S. M. Sze, Appl. Phys. Lett. 9, 242 (1966).

19. S. M. Sze (Private Communication).

20. R.A. Logan and S. M. Sze, Proc. Int. Conf. on Phys. of Semiconductors, Kyoto, Japan, 1966, to be published.

21. C.R.Crowell and S. M.Sze, Solid-State Electron. 8, 979 (1965).

22. S. M. Sze and G. Gibbons, Appl. Phys. Lett. 8, 111 (1966).

23. B. Agusta and R. L. Anderson, J. Appl. Phys. 36, 206 (1965).

24. John L. Moll, Physics of Semiconductors (McGraw-Hill Book Company, Inc., New York, 1964), Chapter 11.

25. H.A. Bethe, NDRC Div. 14 Report, MIT Radiation Lab. No. 43-12, Nov. 23, 1942.

26. Ernest David Courant, Thesis, The University of Rochester (1943).

27. C.R. Crowell, Solid-State Electron. 8, 395 (1965).

28. A. M. Goodman, J. Appl. Phys. 34, 329 (1963).

29. C.A. Mead and W. G. Spitzer, Phys. Rev. 134, A713 (1964).

DOCUMENT CONTROL DATA – R&D

(Security classification of title, body of abstract and indexing annotation must be entered when the overall report is classified)

1. ORIGINATING ACTIVITY *(Corporate author)* Lincoln Laboratory, M.I.T.	2a. REPORT SECURITY CLASSIFICATION Unclassified 2b. GROUP None

3. REPORT TITLE

The GaAs-InSb Graded-Gap Heterojunction

4. DESCRIPTIVE NOTES *(Type of report and inclusive dates)*

Technical Note

5. AUTHOR(S) *(Last name, first name, initial)*

Hinkley, Everett D. Rediker, Robert H.

6. REPORT DATE	7a. TOTAL NO. OF PAGES	7b. NO. OF REFS
15 August 1967	54	29

8a. CONTRACT OR GRANT NO. AF 19(628)-5167 b. PROJECT NO. 649L c. d.	9a. ORIGINATOR'S REPORT NUMBER(S) Technical Note 1967-40 9b. OTHER REPORT NO(S) *(Any other numbers that may be assigned this report)* ESD-TR-67-468

10. AVAILABILITY/LIMITATION NOTICES

This document has been approved for public release and sale; its distribution is unlimited.

11. SUPPLEMENTARY NOTES	12. SPONSORING MILITARY ACTIVITY
None	Air Force Systems Command, USAF

13. ABSTRACT

The interface-alloy technique has been used to produce heterojunctions between GaAs and InSb. X-ray and Kossel line patterns show that, despite the relatively large 14% lattice mismatch between the semiconductors, these heterojunctions are single-crystal. Photocurrent and current-voltage measurements are explained by a model for the heterojunction band structure in which the salient feature is a region of the order of 60 Å long which has a linearly-graded energy gap joining the GaAs to the InSb. In addition, interface states "fix" the location of the GaAs bands at the heterojunction interface such that, at room temperature, the conduction band extrapolates to a value approximately 0.93 eV above the Fermi level. The photocurrent occurs via hot carriers generated in the graded-gap region which traverse this region (with a mean free path of approximately 20 Å) to the heterojunction barrier maximum. As predicted by the model, incident monochromatic radiation of energy smaller than the GaAs bandgap produces a photocurrent which varies exponentially with photon energy as $I_o \exp[C(h\nu - E_g)]$, where C is a positive parameter which decreases for increasing reverse bias on the heterojunction, and I_o is the extrapolated response at the GaAs bandgap, which is independent of applied bias. The forward current of units fabricated with n-type GaAs varies as $\exp(qV/\eta kT)$, and, except at lower temperatures where tunneling becomes important, the values of η as a function of the GaAs impurity doping concentration can be explained in terms of the increase in the heterojunction barrier height with voltage, since part of the depletion layer potential is across the graded-gap region. Similarly, the voltage dependence of the reverse current is quantitatively explained by this model. The results of the capacitance-voltage measurements are consistent with the current-voltage and photocurrent measurements evaluated in terms of the graded-gap heterojunction model.

14. KEY WORDS

gallium arsenide
indium antimonide
graded-gap heterojunction
interface-alloy technique